

Performance Analysis of Intelligent CR-NOMA Model for Industrial IoT Communications

Yinghua Zhang^{1,2}, Jian Liu¹, Yunfeng Peng¹, Yanfang Dong² and Changming Zhao^{3,*}

¹School of Computer and Communication Engineering, University of Science and Technology Beijing, Beijing, 100083, China

²Dawning Information Industry Co., Ltd., Beijing, 100193, China

³School of Computer Science, Chengdu University of Information Technology, Chengdu, 610225, China

*Corresponding Author: Changming Zhao. Email: zcm84@cuit.edu.cn

Received: 01 April 2020; Accepted: 03 May 2020

Abstract: Aiming for ultra-reliable low-latency wireless communications required in industrial internet of things (IIoT) applications, this paper studies a simple cognitive radio non-orthogonal multiple access (CR-NOMA) downlink system. This system consists of two secondary users (SUs) dynamically interfered by the primary user (PU), and its performance is characterized by the outage probability of the SU communications. This outage probability is calculated under two conditions where, a) the transmission of PU starts after the channel state information (CSI) is acquired, so the base station (BS) is oblivious of the interference, and b) when the BS is aware of the PU interference, and the NOMA transmission is adapted to the more comprehensive knowledge of the signal to interference plus noise ratio (SINR). These results are verified by simulations, and their good agreement suggests our calculations can be used to reduce the complexity of future analysis. We find the outage probability is reduced when the SUs move further away from the primary transmitter or when the signal from PU is less powerful, and the BS always has better performance when it is aware of the interference. The findings thus emphasize the importance of monitoring the channel quality and real-time feedback to optimize the performance of CR-NOMA system.

Keywords: Industrial internet of things (IIoT); non-orthogonal multiple access (NOMA); quality of service (QoS); successive interference cancellation (SIC)

1 Introduction

Recently, there is a growing trend in the integration of sensors and sensors based systems with cyber physical system (CPS) and device-to-device (D2D) communications. CPS is a complex system that integrates computation, communication, and physical processes. Recent years the explosion of new technologies such as the internet of things (IoT), cloud computing, machine-to-machine (M2M) communications, 3D printing, and big data has great impacts on industry 4.0 [1]. The fifth generation communication (5G) is on the horizon and IoT would be one of its major applications [2]. The application of IoT in industrial sectors, i.e., the industrial IoT (IIoT), has attracted tremendous attention from governments, academia and industry, for its substantial potential to reshape various industry



This work is licensed under a Creative Commons Attribution 4.0 International License, which permits unrestricted use, distribution, and reproduction in any medium, provided the original work is properly cited.

verticals such as electricity, transportation, healthcare, and manufacturing [3]. A definition of IIoT given by General Electric (GE) refers it as “the network of a multitude of industrial devices connected by communications technologies that results in systems that can monitor, collect, exchange, analyze, and deliver valuable new insights like never before” [4]. Since the communication technologies play a critical role in the IIoT system, there is an emerging consensus on the need to develop ultra-reliable low-latency wireless communication networks, in which the potential of the IIoT can be fully unlocked [5].

However, given the constraints of scarce bandwidth, connecting billions of smart IoT devices with diversified quality of service (QoS) requirements is challenging even in 5G networks [6]. The non-orthogonal multiple access (NOMA) shows great potential in reducing system latency by enabling multiple users to access the same channel simultaneously [7–12], and thus greatly improves the efficiency of transmission and computation. In the applications of IoT, some users may require quick transmission of small packets. To address such requirements, the author in [13] designed a new multiple-input multiple-output non-orthogonal multiple access (MIMO-NOMA) scheme, in which the QoS requirement of one user is strictly fulfilled, and the other users are served opportunistically.

The application of NOMA in IoT system can be particularly fruitful since non-orthogonal access provides uncoordinated communication with strictest requirements in transmission latency. Comprehensive numerical results emphasized that the existing NOMA scheme have achieved higher energy efficiency compared to the conventional orthogonal multiple access (OMA) scheme. Considering the enormous scale of IoT system, the current spectrum efficiency could not meet the requirements of QoS [14–17]. By adjusting the channel characteristics, NOMA might be able to provide a solution that two efficient power allocation policies are adopted to meet the dynamic requirements of QoS, as the attempts made by Haris et al. in [18].

Similarly, the cognitive radio (CR) technology also enables co-existence of primary and secondary users (SUs) in the same frequency band, and results in a more efficient utilization of the limited resource [19,20]. Both the NOMA and the CR technologies thus intend to further improve the spectrum efficiency for transmissions between multiple users, and their combination, CR-NOMA, has attracted considerable interests in recent researches [21–24]. One of the unsolved issues in such attempts is related to the accurate channel state information (CSI) at the transmitter side [25]. To ensure the efficiency of the downlink CR-NOMA system, the CSI is essential so the base station (BS) can perform power allocation strategy among users, which can then determine the correct successive interference cancellation (SIC) order and properly recover the intended information. However, in the case of a cognitive system, the intermittent transmission of the primary users (PU) might bring dynamic interference to the system. The channel quality information (CQI) at the BS could be outdated and fails to match the actual status, resulting in a severe degradation of the system performance. Such dynamic interference must be carefully considered when applying the CR technology to the downlink NOMA transmission systems [26].

In this paper, an intelligent CR-NOMA model under the scenario of IIoT is established where the interference of the PU greatly affects the quality of the secondary transmission channel. In order to match the dynamic CSI and realize ultra-reliable transmission, it is essential for the secondary network to intelligently perceiving the CSI affected by the primary transmission. When the transmit power of the PU is too large or the distance between PU and SU is too small, the outage probability of the secondary user would be greatly affected regardless of the PU interference perceived or not. Therefore, in this paper, we consider two conditions where a) the transmission starts after the acquisition of CSI and feedback of the cognitive users so the BS is oblivious of the dynamic PU interference, and b) the PU keeps steady transmitting during the CSI acquisition and SU communication stages, and the BS is aware of the PU interference and adapts the NOMA transmission according to a more comprehensive signal to interference plus noise ratio (SINR) information. By analyzing the two conditions, we derive the

expressions of outage probability, and the results suggest that NOMA system with interference-oblivious BS achieves higher outage probability than its interference-aware counterpart.

The rest of the paper is structured as follows. Section 2 briefly introduces the proposed system model. Sections 3 and 4 analyze the performance of NOMA systems either oblivious or aware of interference from the primary network. Simulation studies are performed in Section 5, and finally a brief summary is given in Section 6.

2 System Model

Fig. 1 illustrates a typical underlay CR-NOMA downlink system consists of a primary transmitter P , a primary receiver P_0 , a secondary BS S , and multiple secondary receivers U_N . For the SUs, transmission from P could interfere with communications from S , and is thus considered as interference link. In this paper, without loss of generality, we consider a system with two SUs, which can be easily applied to systems with greater complexities.

The signal received at the SU U_k can be expressed as:

$$y_{U_k} = h_k(\sqrt{a_1 E_S} x_1 + \sqrt{a_2 E_S} x_2) + h_{pu_k} \sqrt{E_P} x_p + n_{SU_k} \quad (1)$$

where h_k and h_{pu_k} are the k -th link channel coefficients of U_k from S and P , respectively. a_k is the power allocation coefficient where $a_1 + a_2 = 1$. E_S and E_P are the total transmission power of S and P . x_1 and x_2 are the composite signal from S to each of the two SUs in the model, and x_p is the signal from P to P_0 . n_{SU_k} is the zero-mean additive white Gaussian noise (AWGN) with a variance of σ^2 .

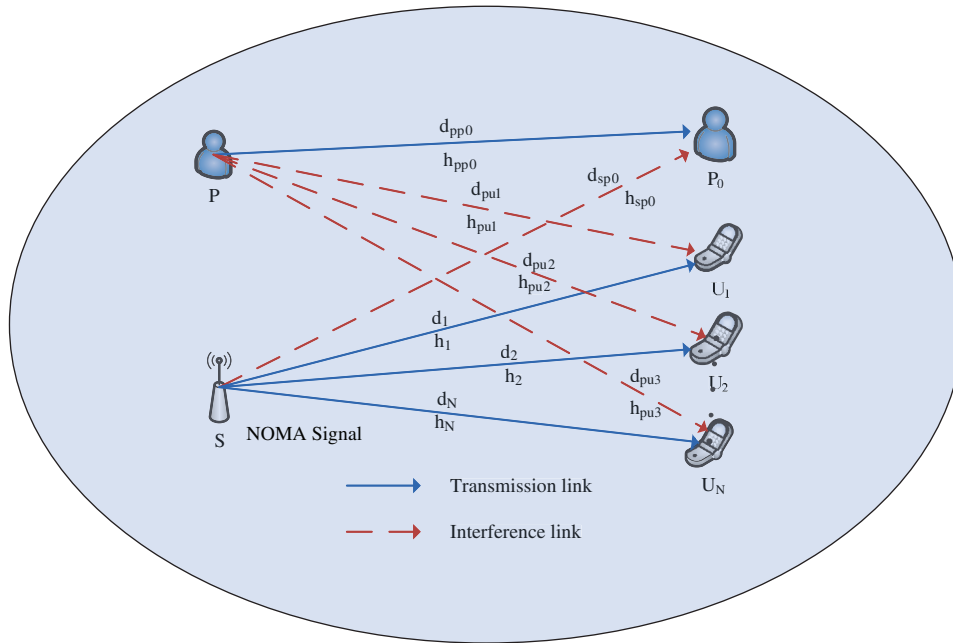


Figure 1: A typical NOMA downlink system in undelay CR network

The channel coefficients h_k and h_{pu_k} are correlative with distance d , and each subjects to exponential distribution of $1/d_{pu_k}^{-\alpha}$ and $1/d_k^{-\alpha}$. α is the path loss exponent, and we define $\Omega_{pu_k} = d_{pu_k}^{-\alpha}$ and $\Omega_k = d_k^{-\alpha}$ in the rest of this work.

The interference from PU is considered to be unpredictable in the secondary transmission model. In the following sections, we respectively analyze the system performance under two conditions: 1) the SUs cannot perceive the interference information of the PU, so such information can be ignored during the analysis; 2) the SUs are capable to perceive the interference information from PU, and the BS adjusts the power allocation coefficients accordingly to optimize the performance of the system. We derive the analytical expressions of outage probability for the two cases, and perform corresponding simulations followed by detailed analysis.

3 NOMA System with Interference-Oblivious Base Station

In a typical CR-NOMA downlink system, the SUs is sorted by the qualities of their channels. The SIC is a technique used by the receiver in a wireless data transmission network that allows decoding of two or more packets arrived simultaneously. By employing SIC technique, the k -th user must firstly demodulate the intended information of the first $k-1$ users properly (whose channel qualities are better), before its own information is demodulated. In this case, the information of the later $N-k$ users (with poor channel qualities) should be regarded as interference.

In this section, we assume that BS is oblivious of the interference of the PU. The SINR and outage probability of U_1 and U_2 are calculated. In one case, U_2 has better channel quality than U_1 , which can be expressed as $|h_1|^2/\sigma^2 < |h_2|^2/\sigma^2$ or $|h_1|^2 < |h_2|^2$ for simplicity. The other case is $|h_1|^2 > |h_2|^2$, the process of calculation is similar and would be skipped to avoid redundancy.

3.1 Calculation of SINR

The signal of U_1 is interfered by U_2 whose channel quality is better. The SINR of the link from S to U_1 would be:

$$\gamma_1 = \frac{a_1 E_S |h_1|^2}{a_2 E_S |h_1|^2 + E_P |h_{pu_1}|^2 + \sigma^2} = \frac{a_1 \gamma_S |h_1|^2}{a_2 \gamma_S |h_1|^2 + \gamma_P |h_{pu_1}|^2 + 1} \quad (2)$$

And the SINR of the link from S to U_2 would be:

$$\gamma_2 = \frac{a_2 E_S |h_2|^2}{E_P |h_{pu_2}|^2 + \sigma^2} = \frac{a_2 \gamma_S |h_2|^2}{\gamma_P |h_{pu_2}|^2 + 1} \quad (3)$$

$$\gamma_{2 \rightarrow 1} = \frac{a_1 E_S |h_2|^2}{a_2 E_S |h_2|^2 + E_P |h_{pu_2}|^2 + \sigma^2} = \frac{a_1 \gamma_S |h_2|^2}{a_2 \gamma_S |h_2|^2 + \gamma_P |h_{pu_2}|^2 + 1} \quad (4)$$

Here, $\gamma_S = E_S/\sigma^2$ and $\gamma_P = E_P/\sigma^2$, representing the system SNR.

3.2 Probability Density Function Analysis

Wireless channel is in the form of electromagnetic wave and can be influenced by various factors. Its numerical expression is typically hard to obtain, except in some specific cases such as urban environments crowded with buildings that work as obstacles. The transmitted signal is scattered by these obstacles, and the received signal would be composed of many independent and identically distributed random signals. The wireless channel response coefficient would be a complex Gaussian random variable, i.e., $h = h_R + jh_I$ and $h \in CN(0, \Omega)$. The coefficient of the fading channel $X = |h|$ subjects to Rayleigh distribution, where the probability density function (PDF) and the cumulative distribution function (CDF) can be written as [27,28]:

$$f_{|h|^2}(x) = \frac{1}{\Omega} e^{-\frac{x}{\Omega}}, x \geq 0 \quad (5)$$

$$F_{|h|^2}(x) = 1 - e^{-\frac{x}{\Omega}}, x \geq 0 \quad (6)$$

3.3 Outage Performance Analysis

For simplicity, we set the target rates $R_1^* = R_2^* = R_c$, and the threshold of secondary SNR is $\gamma_{th} = 2^{R_c} - 1$. When $|h_1|^2 < |h_2|^2$, the outage probability of U_1 and U_2 is given by:

$$\begin{aligned} P_{h_1 < h_2}^{u_1} &= 1 - \Pr\{\gamma_1 > \gamma_{th}, |h_1|^2 < |h_2|^2\} \\ &= 1 - \int_{\Delta_2}^{+\infty} \frac{1}{\Omega_1} e^{\frac{x_1}{\Omega_1}} \left[\int_0^{\Delta_4} \frac{1}{\Omega_{pu_1}} e^{\frac{y_1}{\Omega_{pu_1}}} \left(\int_0^{x_1} \frac{1}{\Omega_2} e^{\frac{x_2}{\Omega_2}} dx_2 \right) dy_1 \right] dx_1 \\ &= 1 - (w_1 - w_2), \frac{a_1}{a_2} > \gamma_{th} \end{aligned} \quad (7)$$

$$\begin{aligned} P_{h_1 < h_2}^{u_2} &= 1 - \Pr\{\gamma_2 > \gamma_{th}, \gamma_{2 \rightarrow 1} < \gamma_{th}, |h_1|^2 < |h_2|^2\} \\ &= \begin{cases} 1 - \int_{\Delta_1}^{+\infty} f_{|h|^2}(x_2) dx_2 \int_0^{\Delta_3} f_{|h|^2}(y_2) dy_2 \int_0^{x_2} f_{|h|^2}(x_1) dx_1, (\frac{a_1}{a_2} > \gamma_{th} + 1) \\ 1 - \int_{\Delta_2}^{+\infty} f_{|h|^2}(x_2) dx_2 \int_0^{\Delta_4} f_{|h|^2}(y_2) dy_2 \int_0^{x_2} f_{|h|^2}(x_1) dx_1, (\gamma_{th} < \frac{a_1}{a_2} < \gamma_{th} + 1) \end{cases} \\ &= \begin{cases} 1 - (w_3 - w_4 + w_5), (\frac{a_1}{a_2} > \gamma_{th} + 1) \\ 1 - (w_6 - w_7 + w_8), (\gamma_{th} < \frac{a_1}{a_2} < \gamma_{th} + 1) \end{cases} \end{aligned} \quad (8)$$

More detailed derivation process can be found in Appendix A. In Eqs. (7) and (8), we have:

$$\begin{aligned} \Delta_1 &= \frac{\gamma_{th}}{a_2 \gamma_S}, & \Delta_2 &= \frac{\gamma_{th}}{(a_1 - a_2 \gamma_{th}) \gamma_S}, \\ \Delta_3 &= \frac{a_2 \gamma_S x_2 - \gamma_{th}}{\gamma_{th} \gamma_P}, & \Delta_4 &= \frac{(a_1 - a_2 \gamma_{th}) \gamma_S x_2 - \gamma_{th}}{\gamma_{th} \gamma_P}, \\ w_1 &= \frac{\Omega_2}{\Omega_1 + \Omega_2} e^{-\frac{\gamma_{th}}{(a_1 - \gamma_{th} a_2) \gamma_S \Omega_1} - \frac{\gamma_{th}}{(a_1 - \gamma_{th} a_2) \gamma_S \Omega_2}}, & w_2 &= \frac{\gamma_P \gamma_{th} \Omega_2 \Omega_{pu_1} e^{-\frac{\gamma_{th}}{(a_1 - \gamma_{th} a_2) \gamma_S \Omega_1} - \frac{\gamma_{th}}{(a_1 - \gamma_{th} a_2) \gamma_S \Omega_2}}}{(\Omega_1 + \Omega_2) \gamma_P \gamma_{th} \Omega_{pu_1} + (a_1 - \gamma_{th} a_2) \gamma_S \Omega_1 \Omega_2}, \\ w_3 &= \frac{a_2 \gamma_S \Omega_2}{a_2 \gamma_S \Omega_2 + \gamma_P \gamma_{th} \Omega_{pu_2}} e^{-\frac{\gamma_{th}}{a_2 \gamma_S \Omega_2}}, & w_4 &= \frac{\Omega_1}{\Omega_1 + \Omega_2} e^{-\frac{\gamma_{th}}{a_2 \gamma_S \Omega_1} - \frac{\gamma_{th}}{a_2 \gamma_S \Omega_2}}, \\ w_5 &= \frac{\gamma_P \gamma_{th} \Omega_1 \Omega_{pu_2} e^{-\frac{\gamma_{th}}{a_2 \gamma_S \Omega_1} - \frac{\gamma_{th}}{a_2 \gamma_S \Omega_2}}}{(\Omega_1 + \Omega_2) \gamma_P \gamma_{th} \Omega_{pu_2} + a_2 \gamma_S \Omega_1 \Omega_2}, & w_6 &= \frac{(a_1 - \gamma_{th} a_2) \gamma_S \Omega_2}{(a_1 - \gamma_{th} a_2) \gamma_S \Omega_2 + \gamma_P \gamma_{th} \Omega_{pu_2}} e^{-\frac{\gamma_{th}}{(a_1 - \gamma_{th} a_2) \gamma_S \Omega_2}}, \\ w_7 &= \frac{\Omega_1}{\Omega_1 + \Omega_2} e^{-\frac{\gamma_{th}}{(a_1 - \gamma_{th} a_2) \gamma_S \Omega_1} - \frac{\gamma_{th}}{(a_1 - \gamma_{th} a_2) \gamma_S \Omega_2}}, & w_8 &= \frac{(a_1 - \gamma_{th} a_2) \gamma_S \Omega_2}{(a_1 - \gamma_{th} a_2) \gamma_S \Omega_2 + \gamma_P \gamma_{th} \Omega_{pu_2}} e^{-\frac{\gamma_{th}}{(a_1 - \gamma_{th} a_2) \gamma_S \Omega_2}}, \end{aligned}$$

The above calculation is based on the condition $|h_1|^2 < |h_2|^2$. In a real system, it is possible to have $|h_1|^2 > |h_2|^2$, and the process of calculation would be similar to Eqs. (7) and (8). Then the final expressions of secondary outage probability, which are used in the simulation study of Section 5, should be:

$$P_{out}^{\mu_1} = P_{h_1 > h_2}^{\mu_1} + P_{h_1 < h_2}^{\mu_1} \quad (9)$$

$$P_{out}^{\mu_2} = P_{h_1 > h_2}^{\mu_2} + P_{h_1 < h_2}^{\mu_2} \quad (10)$$

4 NOMA System with Interference-Aware Base Station

In this section, we consider the condition that the BS perceives the PU interference. We consider the transmission of PU to be continuous and thus the signal of SUs to be interfered during the acquisition of CSI as well as the secondary communication stages. Under this condition, the BS adjusts the power allocation coefficients of the SUs according to more comprehensive channel quality information, so that optimized system performance can be achieved. Again, the following calculation

is under the condition that U_2 has better channel quality, i.e., $\frac{E_S|h_1|^2}{E_P|h_{pu_1}|^2 + \sigma_0^2} < \frac{E_S|h_2|^2}{E_P|h_{pu_2}|^2 + \sigma_0^2}$. When $\frac{E_S|h_1|^2}{E_P|h_{pu_1}|^2 + \sigma_0^2} > \frac{E_S|h_2|^2}{E_P|h_{pu_2}|^2 + \sigma_0^2}$, similar results would be obtained.

4.1 Calculation of SINR

When the secondary users are under the condition of good signal-to-noise ratios, the channel noise σ^2 can be ignored, and the channel gains of U_1 and U_2 would be:

$$g_1 = \frac{E_S|h_1|^2}{E_P|h_{pu_1}|^2} = \frac{\gamma_S|h_1|^2}{\gamma_P|h_{pu_1}|^2} \quad (11)$$

$$g_2 = \frac{E_S|h_2|^2}{E_P|h_{pu_2}|^2} = \frac{\gamma_S|h_2|^2}{\gamma_P|h_{pu_2}|^2} \quad (12)$$

Since the channel quality of U_2 is better than U_1 , we have $g_1 < g_2$, and the SINR can be given as:

$$\begin{aligned} \gamma_1 &= \frac{a_1 g_1}{a_2 g_1 + 1} \\ \gamma_{2 \rightarrow 1} &= \frac{a_1 g_2}{a_2 g_2 + 1} \\ \gamma_2 &= a_2 g_2 \end{aligned} \quad (13)$$

4.2 Probability Density Function Analysis

The channel coefficient $|h|^2$ subjects to exponential distribution and the PDFs of $\gamma_S|h_1|^2$ and $\gamma_P|h_{pu_1}|^2$ are given by:

$$f_{\gamma_S|h_1|^2}(x) = \frac{1}{\gamma_S \Omega_1} e^{-\frac{x}{\gamma_S \Omega_1}}, x \geq 0 \quad (14)$$

$$f_{\gamma_P|h_{pu_1}|^2}(x) = \frac{1}{\gamma_P\Omega_{pu_1}} e^{-\frac{x}{\gamma_P\Omega_{pu_1}}}, x \geq 0 \quad (15)$$

Thus, the CDF of g_1 would be:

$$\begin{aligned} F_{g_1}(z) &= \Pr\left\{\frac{\gamma_S|h_1|^2}{\gamma_P|h_{pu_1}|^2} \leq z\right\} \\ &= \int_0^{+\infty} \frac{1}{\gamma_P\Omega_{pu_1}} e^{-\frac{v}{\gamma_P\Omega_{pu_1}}} dv \int_0^{zv} \frac{1}{\gamma_S\Omega_1} e^{-\frac{w}{\gamma_S\Omega_1}} dw \\ &= 1 - \frac{\gamma_S\Omega_1}{\gamma_S\Omega_1 + z\gamma_P\Omega_{pu_1}} \end{aligned} \quad (16)$$

By taking the differentiation of Eq. (16), we acquire the PDF of g_1 as:

$$f_{g_1}(z) = \frac{\gamma_S\gamma_P\Omega_1\Omega_{pu_1}}{(\gamma_S\Omega_1 + z\gamma_P\Omega_{pu_1})^2} \quad (17)$$

Similarly, we note the PDF of g_2 to be:

$$f_{g_2}(z) = \frac{\gamma_S\gamma_P\Omega_2\Omega_{pu_2}}{(\gamma_S\Omega_2 + z\gamma_P\Omega_{pu_2})^2} \quad (18)$$

4.3 Outage Performance Analysis

If $g_1 < g_2$, the outage probability of U_1 and U_2 would be:

$$\begin{aligned} P_{g_1 < g_2}^{u_1} &= 1 - \Pr\{\gamma_1 > \gamma_{th}, g_1 < g_2\} \\ &= 1 - \int_{\Delta_2}^{+\infty} f_{g_1}(x) dx \int_0^x f_{g_2}(y) dy, \frac{a_1}{a_2} > \gamma_{th} \\ &= 1 - (b_1 b_2 \ln(1 + \frac{z_1}{b_2}) - z_1 b_1), \frac{a_1}{a_2} > \gamma_{th} \end{aligned} \quad (19)$$

$$\begin{aligned} P_{g_1 < g_2}^{u_2} &= 1 - \Pr\{\gamma_2 > \gamma_{th}, \gamma_{2 \rightarrow 1} > \gamma_{th}, g_1 < g_2\} \\ &= \begin{cases} 1 - \int_{\Delta_1}^{+\infty} f_{g_2}(x) dx \int_0^x f_{g_1}(y) dy, \frac{a_1}{a_2} > \gamma_{th} + 1 \\ 1 - \int_{\Delta_2}^{+\infty} f_{g_2}(x) dx \int_0^x f_{g_1}(y) dy, \gamma_{th} < \frac{a_1}{a_2} < \gamma_{th} + 1 \end{cases} \\ &= \begin{cases} 1 - (b_1 b_2 \ln(1 - \frac{z_2}{b_1}) + z_2 b_1), \frac{a_1}{a_2} > \gamma_{th} + 1 \\ 1 - (b_1 b_2 \ln(1 - \frac{z_3}{b_1}) + z_3 b_1), \gamma_{th} < \frac{a_1}{a_2} < \gamma_{th} + 1 \end{cases} \end{aligned} \quad (20)$$

where $f_{g_1}(x)$ and $f_{g_2}(x)$ are given in Eqs. (17) and (18) respectively. Please refer to Appendix B for detailed derivation processes. The other parameters in Eqs. (19) and (20) are written as follows:

$$\begin{aligned}\Delta_1 &= \frac{\gamma_{th}}{a_2 \gamma_s}, & \Delta_2 &= \frac{\gamma_{th}}{(a_1 - a_2 \gamma_{th}) \gamma_s}, \\ b_1 &= \frac{\Omega_2 \Omega_{pu_1}}{\Omega_2 \Omega_{pu_1} - \Omega_1 \Omega_{pu_2}}, & b_2 &= \frac{\Omega_1 \Omega_{pu_2}}{\Omega_2 \Omega_{pu_1} - \Omega_1 \Omega_{pu_2}}, \\ z_1 &= \frac{(a_1 - \gamma_{th} a_2) \gamma_s \Omega_1}{(a_1 - \gamma_{th} a_2) \gamma_s \Omega_1 + \gamma_{th} \gamma_P \Omega_{pu_1}}, & z_2 &= \frac{a_2 \gamma_s \Omega_2}{a_2 \gamma_s \Omega_2 + \gamma_{th} \gamma_P \Omega_{pu_2}}, \\ z_3 &= \frac{(a_1 - \gamma_{th} a_2) \gamma_s \Omega_2}{(a_1 - \gamma_{th} a_2) \gamma_s \Omega_2 + \gamma_{th} \gamma_P \Omega_{pu_2}}.\end{aligned}$$

Again, when $g_1 > g_2$, the results would be similar with $g_1 < g_2$ in the above analysis. Take both cases into account and we have:

$$P_{out}^{u_1} = P_{g_1 > g_2}^{u_1} + P_{g_1 < g_2}^{u_1} \quad (21)$$

$$P_{out}^{u_2} = P_{g_1 > g_2}^{u_2} + P_{g_1 < g_2}^{u_2} \quad (22)$$

5 Simulation and Analysis

According to the analysis above, when the transmission power of PU is too large or the distance between PU and SUs is too small, the outage probability of the SUs will be greatly increased, regardless of the interference of PU perceived or not. Although the interference of PU is a major concern, there are many other factors to be considered, such as target transmission rates of SUs, the SNR of secondary system, and the distances between transmitter and receiver, etc. Monte Carlo simulations are performed to evaluate the performance of secondary outage probability. The simulation results are obtained after 10^5 independent trials.

In this section, we have simulated the outage performance of a NOMA scheme with two SUs affected by dynamic interference from PU. During the simulation process, the system parameters are set as follows: the distance from S to U_1 is $d_1 = 20$ m, and distance from S to U_2 is $d_2 = 25$ m, the path loss factor is set as $\alpha = 2$. The power allocation coefficients of SUs are set as 0.2 and 0.8 respectively. The SNR of PU is defined as γ_P and γ_S represents the SNR of SU. The target rates of two SUs are defined as R_1^* and R_2^* .

Fig. 2 illustrates that the performance of secondary system improves with the increase of γ_S , and the simulation results are well consistent with the theoretical estimates. Additionally, the target transmission rate also affects the secondary outage performance due to different requirements of the quality of the channel. As can be seen, the requirement of higher transmission rate deteriorates the outage performance of SUs.

Fig. 3 shows the analytical results of the outage performance of the NOMA protocol varied with different γ_P . When the transmission power of PU increases to $\gamma_P = 40$ dB, the secondary outage probability would be larger than 0.1, which means the secondary system can hardly establish normal communications. Thus, the proposed intelligent scheme can be more effective under the condition that transmission power of PU is in a moderate level.

Secondly, in Fig. 4, we analyze the secondary outage probability vs. γ_S when the primary interference is perceived. As can be seen, the secondary outage probability decreases with the increase of γ_S . Under the condition of higher SNR, the simulation result is consistent well with theoretical computation. In addition, when the interference from the primary user is perceived, the secondary system can obtain more detailed channel information and adjust power allocation strategy of the secondary transmitter to achieve better outage performance following an optimal SIC sequence. On the contrary, without perceiving

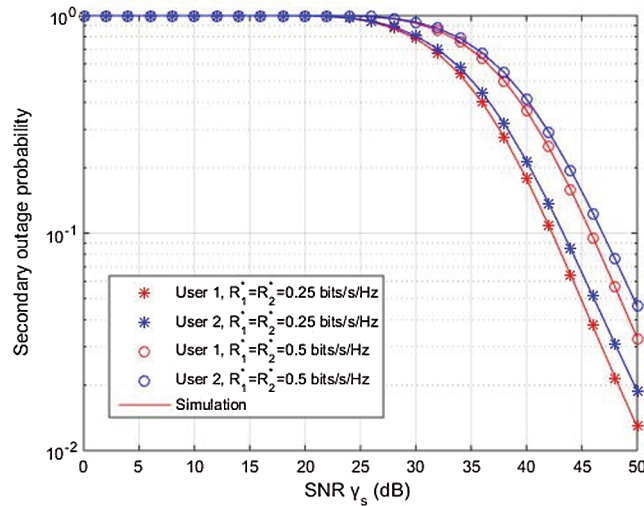


Figure 2: Outage probability of the secondary system compared to the system SNR, when the primary interference is NOT perceived. We assume $d_{pu_1} = d_{pu_2} = 10\text{ m}$, $\gamma_P = 30\text{ dB}$, and the cases when $R_1^* = R_2^* = 0.25$ and 0.5 bits/s/Hz are analyzed

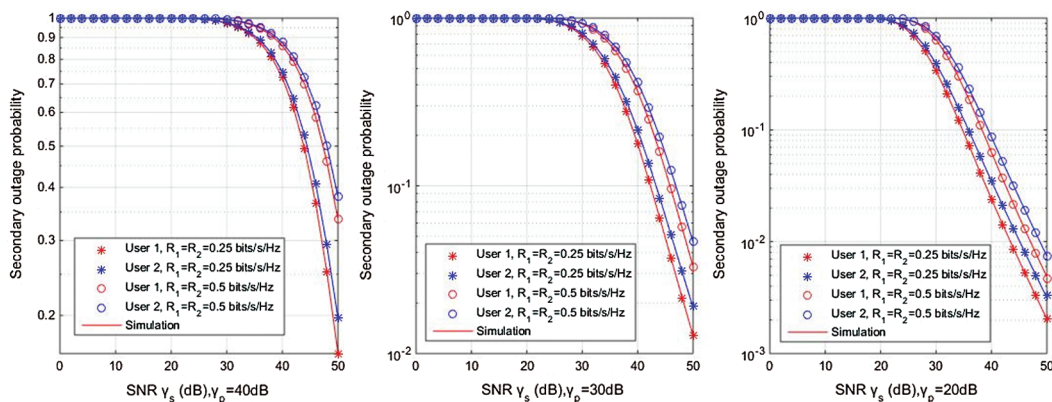


Figure 3: Outage probability of the secondary system compared to the system SNR for different $\gamma_P = E_P/\sigma^2$, when the primary interference is NOT perceived. During the simulation, we set $\gamma_P = 20\text{ dB}, 30\text{ dB}, 40\text{ dB}$, respectively. The other parameters remain the same as in Fig. 2

interference from the PU, the secondary users may possess outdated channel information and could not match the real-time channel status, which deteriorates the outage performance.

Then, the relationship between the probability of secondary outage and the distance of the PU is analyzed in Fig. 5. It can be seen that when the transmission distance increases, the secondary outage probability decreases. Regardless of the PU interference perceived or not, the outage probability is always unsatisfactory when the SU is close to the PU.

From the comparison of Fig. 6, it can be seen that a proper distance should be kept between the SU and the PU to avoid severe interference. When the distance between the SU and the PU increases from 10 meters to 50 meters, the outage probability can be greatly decreased.

Figs. 5 and 6 jointly show the difference of secondary outage performance when the interference of PU is perceived by the SUs. It is obvious that the secondary outage performance is improved when the

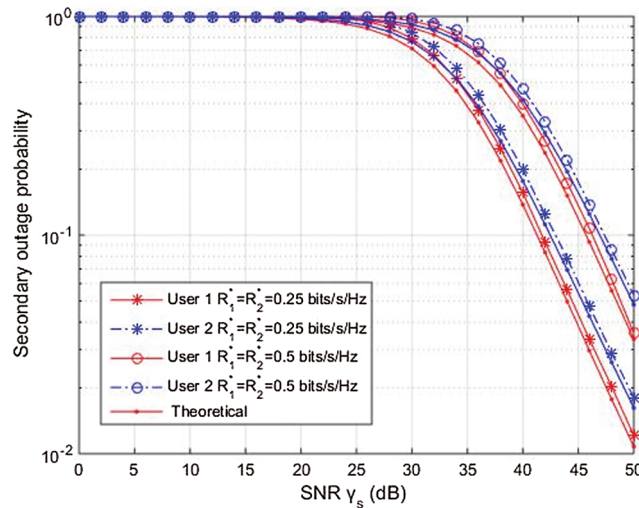


Figure 4: Outage probability of the secondary system compared to the system SNR, under the condition when the primary interference is perceived. During the simulation, we set $d_{pu_1} = d_{pu_2} = 10\text{ m}$, $\gamma_p = 30\text{ dB}$, and the cases $R_1^* = R_2^* = 0.25$ and 0.5 bits/s/Hz are analyzed

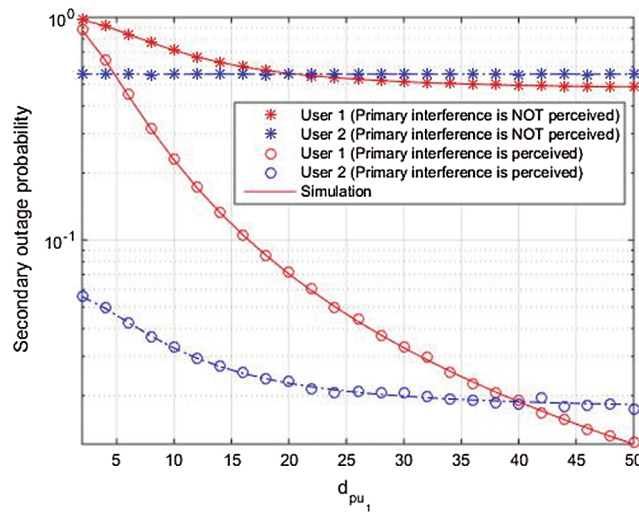


Figure 5: Outage probability for the secondary system compared to the distance between the primary transmitter and the SU U_1 . The simulation parameters are set to $\gamma_S = \gamma_P = 30\text{ dB}$, $R_1^* = R_2^* = 0.25$ bits/s/Hz. While d_{pu_1} is the variable in the simulation, we fix d_{pu_2} to 10 m and thus the outage probability is constant when the primary interference is not perceived

interference from PU has been perceived. The key idea of this feature is that the secondary system can obtain more detailed channel information through perceiving interference from PU, and thus properly adjusts power allocation coefficients of the secondary transmitter and recovers information following an optimal SIC sequence. Therefore, in the cognitive downlink NOMA system, it is essential to take the interference information of PU into account when analyzing performance of secondary networks.

Fig. 7 shows the outage probability when the SUs move away from the transmitter. Set $d_{pu_1} = d_{pu_2}$ and $\gamma_S = \gamma_P = 30\text{ dB}$ in this process and other parameters remain the same as in Fig. 5. The outage probability is greatly reduced when the SUs move away from the PU. As the changes of d_{pu_1} and d_{pu_2} would not affect the

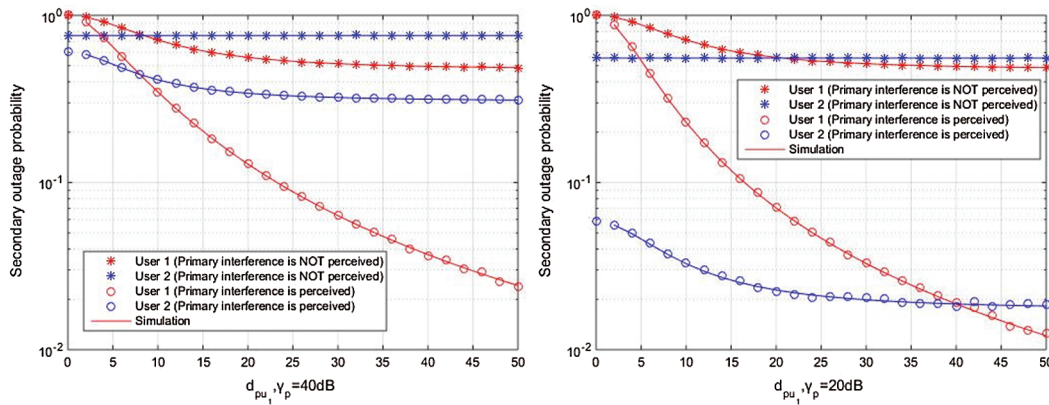


Figure 6: Outage probability for the secondary system compared to the distance between the primary transmitter and the secondary user U_1 for different d_{pu_1} . During the simulation, we set $d_{pu_1} = 10\text{ m}, 50\text{ m}$, respectively. Other parameters remain unchanged as in Fig. 5

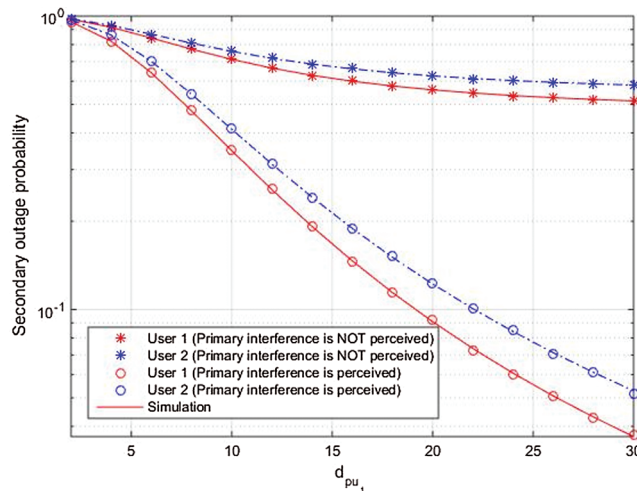


Figure 7: Outage probability for the secondary system compared to the distance between the primary transmitter and the SUs

SIC sequence and the channel status always matches with real-time status, the secondary outage performance under such condition would always be better than that the interference is not perceived.

Lastly, as shown in Fig. 8, we compare the secondary outage probability with different γ_p . Set $d_{pu_1} = d_{pu_2} = 10\text{ m}$, $\gamma_S = 30\text{ dB}$, and $R_1^* = R_2^* = 0.5\text{ bits/s/Hz}$.

Fig. 8 shows the trend of secondary outage probability with the variation of γ_p , considering the interference from the primary transmitter perceived or not. The theoretical numerical analysis is consistent with the simulation results. As is shown in the plot, the outage probability of the first case (when the SUs do not perceive the primary interference) is significantly higher than the second case (when the primary interference is perceived). But the improvement is less significant at large γ_p because the minimal requirement of transmission cannot be matched. In the second case, the SUs can obtain the accurate CSI in time and adjust the power allocation coefficient, so that the SINR of the secondary system can be optimized. However, in the first case, the SUs could not perceive the interference, and the secondary outage probability is seriously degraded because the channel information obtained by the SUs

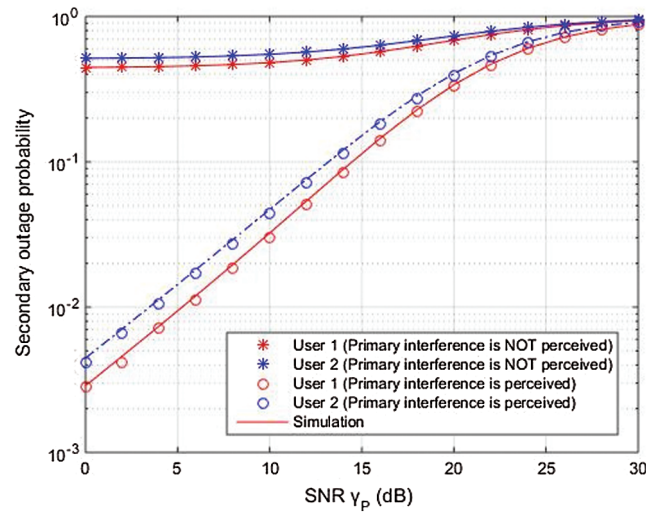


Figure 8: Outage probability for the secondary system compared to the transmit power from the PU. By perceiving the interference from the PU, the outage risk can be reduced, but the difference becomes limited when the PU signal is too strong

mismatch the current channel state. Therefore, it is rather meaningful for the secondary systems to dynamically perceive the interference from PU and adapt to a more accurate channel state to achieve better wireless communications.

6 Conclusions

In this paper, in order to achieve ultra-reliable wireless communications required in critical IIoT applications, we proposed a CR-NOMA model that consists of two SUs and a PU. The outage probability of the system is analyzed under the following two conditions:

- a) The BS is oblivious of the primary interference, corresponding to when the transmission of PU started after the CSI acquisition and feedback stage of the cognitive users;
- b) The BS is aware of the primary interference, and PU keeps its transmission during both stages of CSI acquisition and communication of secondary system.

The results of these theoretical calculations have been compared to simulation experiments and indicate a well-matched effect. The simulation results suggest that the outage probability is closely associated with the distance between the SUs and the primary transmitter, and the power allocation strategy of the primary transmitter. Compared to interference-oblivious BS, the outage probability is greatly reduced when the NOMA transmission is carried out by interference-aware BS. Dynamic acquisition of the real channel condition would improve the performance of the NOMA system. The results emphasize the importance to apply continuous channel quality monitoring, real-time feedback, and advanced spectrum sensing in the CR-NOMA system, which motives technology improvements in IIoT scenarios.

Funding Statement: This work is funded by National Major Project (No. 2017ZX03001021-005), National Key R & D Program of China (No. 2017YFB1001600), Standard Development and Test bed Construction for Smart Factory Virtual Mapping Model and Digitized Delivery (No. MIIT 2019-00899-3-1) and 2018 Sugon Intelligent Factory on Advanced Computing Devices (No. MIIT 2018-265-137).

Conflicts of Interest: The authors declare that they have no conflicts of interest to report regarding the present study.

References

1. Wang, L., Wang, G. (2016). Big data in cyber-physical systems, digital manufacturing and industry 4.0. *International Journal of Engineering and Manufacturing*, 6(4), 1–8.
2. Ejaz, W., Anpalagan, A., Imran, M. A., Jo, M., Muhammad, N. et al. (2016). Internet of things (IoT) in 5G wireless communications. *IEEE Access*, 4, 10310–10314. DOI 10.1109/ACCESS.2016.2646120.
3. Xu, L. D., He, W., Li, S. (2014). Internet of things in industries: a survey. *IEEE Transactions on Industrial Informatics*, 10(4), 2233–2243. DOI 10.1109/TII.2014.2300753.
4. GE Digital (2020). Everything you need to know about the industrial internet of things. <https://www.ge.com/digital/blog/everything-you-need-know-about-industrial-internet-things>.
5. Chen, H., Dong, Z., Vucetic, B. (2019). Non-coherent and non-orthogonal massive SIMO for critical industrial IoT communications. *IEEE International Conference on Industrial Cyber Physical Systems*, pp. 436–441. Taipei.
6. NGMN Alliance (2015). *NGMN 5G white paper*, 11–16.
7. Do, D. T., Le, C. B. (2018). Application of NOMA in wireless system with wireless power transfer scheme: outage and ergodic capacity performance analysis. *Sensors*, 18(10), 3501. DOI 10.3390/s18103501.
8. Lv, L., Chen, J., Ni, Q., Ding, Z. (2017). Design of cooperative non-orthogonal multicast cognitive multiple access for 5G systems: user scheduling and performance analysis. *IEEE Transactions on Communications*, 65(6), 2641–2656. DOI 10.1109/TCOMM.2017.2677942.
9. Arzykulov, S., Tsiftsis, T. A., Nauryzbayev, G., Abdallah, M. M. (2019). Outage performance of cooperative underlay CR-NOMA with imperfect CSI. *IEEE Communications Letters*, 23(1), 176–179. DOI 10.1109/LCOMM.2018.2878730.
10. Chen, Y., Wang, L., Jiao, B. (2017). Cooperative multicast non-orthogonal multiple access in cognitive radio. *IEEE International Conference on Communications*, pp. 1–6. Paris.
11. Zhang, Y., Ge, J. (2017). Performance analysis for non-orthogonal multiple access in energy harvesting relaying networks. *IET Communications*, 11(11), 1768–1774. DOI 10.1049/iet-com.2016.1442.
12. Liu, M., Song, T., Gui, G. (2018). Deep cognitive perspective: resource allocation for NOMA based heterogeneous IoT with imperfect SIC. *IEEE Internet of Things Journal*, 6(2), 2885–2894. DOI 10.1109/JIOT.2018.2876152.
13. Ding, Z., Dai, L., Poor, H. V. (2016). MIMO-NOMA design for small packet transmission in the internet of things. *IEEE Access*, 4, 1393–1405. DOI 10.1109/ACCESS.2016.2551040.
14. Borkar, S., Pande, H. (2016). Application of 5G next generation network to internet of things. *International Conference on Internet of Things and Applications*, pp. 443–447. Pune.
15. Lv, T., Ma, Y., Zeng, J., Mathiopoulos, P. T. (2018). Millimeter-wave NOMA transmission in cellular M2M communications for internet of things. *IEEE Internet of Things Journal*, 5(3), 1989–2000. DOI 10.1109/JIOT.2018.2819645.
16. Chinnadurai, S., Yoon, D. (2018). Energy efficient MIMO-NOMA HCN with IoT for wireless communication systems. *International Conference on Information and Communication Technology Convergence*, pp. 856–859. Jeju.
17. Lv, L., Chen, J., Ni, Q. (2016). Cooperative non-orthogonal multiple access in cognitive radio. *IEEE Communications Letters*, 20(10), 2059–2062. DOI 10.1109/LCOMM.2016.2596763.
18. Reddy, M. H., Rebekka, B. (2018). Power allocation policies for QoS satisfaction in IoT using NOMA. *2nd International Conference on Trends in Electronics and Informatics*, pp. 576–581. Tirunelveli.
19. Mitola, J. I. (1999). Cognitive radio for flexible mobile multimedia communications. *1999 IEEE International Workshop on Mobile Multimedia Communications (MoMuC'99) (Cat. No. 99EX384)*, pp. 3–10. San Diego, CA, USA.
20. Toutouh, J., Alba, E. (2011). An efficient routing protocol for green communications in vehicular ad-hoc networks. *Genetic and Evolutionary Computation Conference, GECCO'11—Companion Publication*, pp. 719–726. Dublin.
21. Liu, X., Wang, Y., Liu, S., Meng, J. (2018). Spectrum resource optimization for NOMA-based cognitive radio in 5G communications. *IEEE Access*, 6, 24904–24911. DOI 10.1109/ACCESS.2018.2828801.
22. Ding, Z., Fan, P., Poor, H. V. (2015). Impact of user pairing on 5G non-orthogonal multiple-access downlink transmissions. *IEEE Global Communications Conference*, pp. 1–5. San Diego, CA.

23. Meshgi, H., Zhao, D. (2016). Power allocation and transmission scheduling for a network with bidirectional relaying links. *Wireless Communications and Mobile Computing*, 16(10), 1221–1237. DOI 10.1002/wcm.2600.
24. Meylani, L., Kurniawan, A., Arifianto, M. S. (2019). Radio resource allocation with the fairness metric for low density signature OFDM in underlay cognitive radio networks. *Sensors*, 19(8), 1921. DOI 10.3390/s19081921.
25. Benjebbour, A., Saito, Y., Kishiyama, Y., Li, A., Harada, A. et al. (2013). Concept and practical considerations of non-orthogonal multiple access (NOMA) for future radio access. *International Symposium on Intelligent Signal Processing and Communication Systems*, pp. 770–774. Naha.
26. Qiu, T., Qiao, R., Wu, D. O. (2018). EABS: an event-aware backpressure scheduling scheme for emergency internet of things. *IEEE Transactions on Mobile Computing*, 17(1), 72–84. DOI 10.1109/TMC.2017.2702670.
27. David, H. A., Nagaraja, H. N. (2003). *Order statistics*. Third Edition. New York: John Wiley & Sons, Inc.
28. Yang, Z., Ding, Z., Fan, P., Karagiannidis, G. K. (2016). On the performance of non-orthogonal multiple access systems with partial channel information. *IEEE Transactions on Communications*, 64(2), 654–667. DOI 10.1109/TCOMM.2015.2511078.

Appendix A

Derivation of Eqs. (7) and (8) are as follows:

For the sake of brevity, we define the following parameters $x_1 = |h_1|^2$, $y_1 = |h_{pu_1}|^2$, $x_2 = |h_2|^2$, $y_2 = |h_{pu_2}|^2$, and the probability density function can be written as $f(x_1)$, $f(y_1)$, $f(x_2)$ and $f(y_2)$. It is obvious that random variables x_1 , y_1 , x_2 and y_2 respectively subjects to independent and identically exponential distribution, and the rate parameters are noted as Ω_1 , Ω_{pu_1} , Ω_2 and Ω_{pu_2} . In addition, we define $c = \frac{a_1}{a_2}$, $\Delta_1 = \frac{\gamma_{th}}{a_2\gamma_S}$, $\Delta_2 = \frac{\gamma_{th}}{(a_1 - a_2\gamma_{th})\gamma_S}$, $\Delta_3 = \frac{(a_1 - a_2\gamma_{th})\gamma_S x_1 - \gamma_{th}}{\gamma_{th}\gamma_P}$, $\Delta_4 = \frac{(a_1 - a_2\gamma_{th})\gamma_S x_2 - \gamma_{th}}{\gamma_{th}\gamma_P}$, $\Delta_{y_3} = \frac{a_2\gamma_S x_2 - \gamma_{th}}{\gamma_{th}\gamma_P}$.

Thus, the outage probability under the condition of $|h_1|^2 < |h_2|^2$ can be expressed as:

$$\begin{aligned}
 P_{h_1 < h_2}^{u_1} &= 1 - \Pr\{\gamma_1 > \gamma_{th}, |h_1|^2 < |h_2|^2\} \\
 &= 1 - \Pr\left\{\frac{a_1\gamma_S|h_1|^2}{a_2\gamma_S|h_1|^2 + \gamma_P|h_{pu_1}|^2 + 1} > \gamma_{th}, |h_1|^2 < |h_2|^2\right\} \\
 &= 1 - \Pr\left\{|h_1|^2 > \frac{\gamma_{th}(\gamma_P|h_{pu_1}|^2 + 1)}{(a_1 - a_2\gamma_{th})\gamma_S}, |h_1|^2 < |h_2|^2\right\} \\
 &= 1 - \int_{\Delta_2}^{+\infty} \frac{1}{\Omega_1} e^{-\frac{x_1}{\Omega_1}} \left[\int_0^{\Delta_3} \frac{1}{\Omega_{pu_1}} e^{-\frac{y_1}{\Omega_{pu_1}}} \left(\int_0^{x_1} \frac{1}{\Omega_2} e^{-\frac{x_2}{\Omega_2}} dx_2 \right) dy_1 \right] dx_1
 \end{aligned} \tag{23}$$

$$\begin{aligned}
 P_{h_1 < h_2}^{\mu_2} &= 1 - \Pr\{\gamma_2 > \gamma_{th}, \gamma_{2 \rightarrow 1} > \gamma_{th}, |h_1|^2 < |h_2|^2\} \\
 &= 1 - \Pr\left\{\frac{a_2 \gamma_S |h_2|^2}{\gamma_P |h_{pu_2}|^2 + 1} > \gamma_{th}, \frac{a_1 \gamma_S |h_2|^2}{a_2 \gamma_S |h_2|^2 + \gamma_P |h_{pu_2}|^2 + 1} > \gamma_{th}, |h_1|^2 < |h_2|^2\right\} \\
 &= \Pr\left\{x_2 > \frac{\gamma_{th}(\gamma_P \gamma_2 + 1)}{a_2 \gamma_S}, x_2 > \frac{\gamma_{th}(\gamma_P \gamma_2 + 1)}{(a_1 - a_2 \gamma_{th}) \gamma_S}, x_1 < x_2\right\} \\
 &= \begin{cases} 1 - \int_{\Delta_1}^{+\infty} f(x_2) dx_2 \int_0^{\Delta_3} f(y_2) dy_2 \int_0^{x_2} f(x_1) dx_1, c > \gamma_{th} + 1 \\ 1 - \int_{\Delta_2}^{+\infty} f(x_2) dx_2 \int_0^{\Delta_4} f(y_2) dy_2 \int_0^{x_2} f(x_1) dx_1, \gamma_{th} < c < \gamma_{th} + 1 \end{cases}
 \end{aligned} \tag{24}$$

If $c > \gamma_{th} + 1$, $P_{h_1 < h_2}^{\mu_2}$ can be calculated as

$$\begin{aligned}
 P_{h_1 < h_2}^{\mu_2} &= 1 - \int_{\Delta_1}^{+\infty} f(x_2) dx_2 \int_0^{\frac{a_2 \gamma_S x_2 - \gamma_{th}}{\gamma_{th} \gamma_P}} f(y_2) dy_2 \int_0^{x_2} f(x_1) dx_1 \\
 &= 1 - \int_{\Delta_1}^{+\infty} \frac{1}{\Omega_2} e^{-\frac{x_2}{\Omega_2}} dx_2 \int_0^{\frac{a_2 \gamma_S x_2 - \gamma_{th}}{\gamma_{th} \gamma_P}} \frac{1}{\Omega_{pu_2}} e^{-\frac{y_2}{\Omega_{pu_2}}} dy_2 \int_0^{x_2} \frac{1}{\Omega_1} e^{-\frac{x_1}{\Omega_1}} dx_1 \\
 &= 1 - \int_{\Delta_1}^{+\infty} \frac{1}{\Omega_2} e^{-\frac{x_2}{\Omega_2}} dx_2 \int_0^{\frac{a_2 \gamma_S x_2 - \gamma_{th}}{\gamma_{th} \gamma_P}} \frac{1}{\Omega_{pu_2}} e^{-\frac{y_2}{\Omega_{pu_2}}} (1 - e^{-\frac{y_2}{\Omega_1}}) dy_2 \\
 &= 1 - \int_{\Delta_1}^{+\infty} \frac{1}{\Omega_2} e^{-\frac{x_2}{\Omega_2}} \left(1 - \frac{1}{\Omega_{pu_2}} e^{-\frac{a_2 \gamma_S x_2 - \gamma_{th}}{\gamma_{th} \gamma_P \Omega_{pu_2}}}\right) (1 - e^{-\frac{x_2}{\Omega_1}}) dx_2 \\
 &= 1 - \int_{\Delta_1}^{+\infty} \frac{1}{\Omega_2} \left(e^{-\frac{x_2}{\Omega_2}} - e^{-\frac{x_2}{\Omega_2} - \frac{x_2}{\Omega_1}} - e^{-\frac{x_2}{\Omega_2} - \frac{a_1 \gamma_S x_1 - \gamma_{th}}{\gamma_{th} \gamma_P \Omega_{pu_1}}} + e^{-\frac{x_2}{\Omega_2} - \frac{x_2}{\Omega_1} - \frac{a_2 \gamma_S x_2 - \gamma_{th}}{\gamma_{th} \gamma_P \Omega_{pu_2}}}\right) dx_2 \\
 &= 1 - (w_1 - w_2 + w_3)
 \end{aligned} \tag{25}$$

If not, that is for $\gamma_{th} < c < \gamma_{th} + 1$, $P_{h_1 < h_2}^{\mu_2}$ can be calculated as

$$\begin{aligned}
P_{h_1 < h_2}^{u_2} &= 1 - \int_{\Delta_2}^{+\infty} f(x_2) dx_2 \int_0^{\Delta_4} f(y_2) dy_2 \int_0^{x_2} f(x_1) dx_1 \\
&= 1 - \int_{\Delta_2}^{+\infty} \frac{1}{\Omega_2} e^{-\frac{x_2}{\Omega_2}} dx_2 \int_0^{\Delta_4} \frac{1}{\Omega_{pu_2}} e^{-\frac{y_2}{\Omega_{pu_2}}} dy_2 \int_0^{x_2} \frac{1}{\Omega_1} e^{-\frac{x_1}{\Omega_1}} dx_1 \\
&= 1 - \int_{\Delta_2}^{+\infty} \frac{1}{\Omega_2} e^{-\frac{x_2}{\Omega_2}} dx_2 \int_0^{\Delta_4} \frac{1}{\Omega_{pu_2}} e^{-\frac{y_2}{\Omega_{pu_2}}} (1 - e^{-\frac{y_2}{\Omega_1}}) dy_2 \\
&= 1 - \int_{\Delta_2}^{+\infty} \frac{1}{\Omega_2} e^{-\frac{x_2}{\Omega_2}} (1 - \frac{1}{\Omega_{pu_2}} e^{-\frac{\Delta_4}{\Omega_{pu_2}}}) (1 - e^{-\frac{x_2}{\Omega_1}}) dx_2 \\
&= 1 - \int_{\Delta_2}^{+\infty} \frac{1}{\Omega_2} (e^{-\frac{x_2}{\Omega_2}} - e^{-\frac{x_2}{\Omega_2} - \frac{x_2}{\Omega_1}} - e^{-\frac{x_2}{\Omega_2} - \frac{\Delta_4}{\Omega_{pu_1}}} + e^{-\frac{x_2}{\Omega_2} - \frac{x_2}{\Omega_1} - \frac{\Delta_4}{\Omega_{pu_2}}}) dx_2 \\
&= 1 - (w_4 - w_5 + w_6)
\end{aligned} \tag{26}$$

If $c > \gamma_{th}$, the probability of U_1 would be given as:

$$\begin{aligned}
P_{h_1 < h_2}^{u_1} &= 1 - \int_{\Delta_2}^{+\infty} f(x_1) dx_1 \int_0^{\Delta_3} f(y_1) dy_1 \int_{x_1}^{+\infty} f(x_2) dx_2 \\
&= 1 - \int_{\Delta_2}^{+\infty} \frac{1}{\Omega_1} e^{\frac{x_1}{\Omega_1}} \left[\int_0^{\Delta_3} \frac{1}{\Omega_{pu_1}} e^{\frac{y_1}{\Omega_{pu_1}}} \left(\int_{x_1}^{+\infty} \frac{1}{\Omega_2} e^{\frac{x_2}{\Omega_2}} dx_2 \right) dy_1 \right] dx_1 \\
&= 1 - \int_{\Delta_2}^{+\infty} \frac{1}{\Omega_1} e^{\frac{x_1}{\Omega_1}} dx_1 \int_0^{\frac{(a_1 - a_2 \gamma_{th}) \gamma_{th} \gamma_P}{\gamma_{th} \gamma_P}} \frac{1}{\Omega_{pu_1}} e^{\frac{y_1}{\Omega_{pu_1}}} e^{-\frac{x_1}{\Omega_2}} dy_1 \\
&= 1 - \int_{\Delta_2}^{+\infty} \frac{1}{\Omega_2} e^{\frac{x_2}{\Omega_2}} (1 - \frac{1}{\Omega_{pu_2}} e^{\frac{(a_1 - a_2 \gamma_{th}) \gamma_{th} \gamma_P}{\gamma_{th} \gamma_P \Omega_{pu_2}}}) e^{-\frac{x_2}{\Omega_2}} dx_2 \\
&= 1 - \int_{\Delta_2}^{+\infty} \frac{1}{\Omega_1} (e^{-\frac{x_1}{\Omega_2} - \frac{x_1}{\Omega_1}} - e^{-\frac{x_1}{\Omega_2} - \frac{x_1}{\Omega_1} - \frac{(a_1 - a_2 \gamma_{th}) \gamma_{th} \gamma_P}{\gamma_{th} \gamma_P \Omega_{pu_1}}}) dx_1 \\
&= 1 - (w_7 - w_8)
\end{aligned} \tag{27}$$

In the above equations, we have:

$$\begin{aligned}
 w_1 &= \frac{a_2 \gamma_S \Omega_2}{a_2 \gamma_S \Omega_2 + \gamma_P \gamma_{th} \Omega_{pu_2}} e^{-\frac{\gamma_{th}}{a_2 \gamma_S \Omega_2}}, & w_2 &= \frac{\Omega_1}{\Omega_1 + \Omega_2} e^{-\frac{\gamma_{th}}{a_2 \gamma_S \Omega_1} - \frac{\gamma_{th}}{a_2 \gamma_S \Omega_2}}, \\
 w_3 &= \frac{\gamma_P \gamma_{th} \Omega_1 \Omega_{pu_2} e^{-\frac{\gamma_{th}}{a_2 \gamma_S \Omega_1} - \frac{\gamma_{th}}{a_2 \gamma_S \Omega_2}}}{(\Omega_1 + \Omega_2) \gamma_P \gamma_{th} \Omega_{pu_2} + a_2 \gamma_S \Omega_1 \Omega_2}, & w_4 &= \frac{(a_1 - \gamma_{th} a_2) \gamma_S \Omega_2}{(a_1 - \gamma_{th} a_2) \gamma_S \Omega_2 + \gamma_P \gamma_{th} \Omega_{pu_2}} e^{-\frac{\gamma_{th}}{(a_1 - \gamma_{th} a_2) \gamma_S \Omega_2}}, \\
 w_5 &= \frac{\Omega_1}{\Omega_1 + \Omega_2} e^{-\frac{\gamma_{th}}{(a_1 - \gamma_{th} a_2) \gamma_S \Omega_1} - \frac{\gamma_{th}}{(a_1 - \gamma_{th} a_2) \gamma_S \Omega_2}}, & w_6 &= \frac{(a_1 - \gamma_{th} a_2) \gamma_S \Omega_2}{(a_1 - \gamma_{th} a_2) \gamma_S \Omega_2 + \gamma_P \gamma_{th} \Omega_{pu_2}} e^{-\frac{\gamma_{th}}{(a_1 - \gamma_{th} a_2) \gamma_S \Omega_2}}, \\
 w_7 &= \frac{\Omega_2}{\Omega_1 + \Omega_2} e^{-\frac{\gamma_{th}}{(a_1 - \gamma_{th} a_2) \gamma_S \Omega_1} - \frac{\gamma_{th}}{(a_1 - \gamma_{th} a_2) \gamma_S \Omega_2}}, & w_8 &= \frac{\gamma_P \gamma_{th} \Omega_2 \Omega_{pu_1} e^{-\frac{\gamma_{th}}{(a_1 - \gamma_{th} a_2) \gamma_S \Omega_1} - \frac{\gamma_{th}}{(a_1 - \gamma_{th} a_2) \gamma_S \Omega_2}}}{(\Omega_1 + \Omega_2) \gamma_P \gamma_{th} \Omega_{pu_1} + (a_1 - \gamma_{th} a_2) \gamma_S \Omega_1 \Omega_2}.
 \end{aligned}$$

In summary, the outage probability of secondary users can be written as:

$$P_{h_1 < h_2}^{u_1} = 1 - (w_7 - w_8), c > \gamma_{th} + 1 \tag{28}$$

$$P_{h_1 < h_2}^{u_2} = \begin{cases} 1 - (w_1 - w_2 + w_3), c > \gamma_{th} + 1 \\ 1 - (w_4 - w_5 + w_6), \gamma_{th} < c < \gamma_{th} + 1 \end{cases} \tag{29}$$

Appendix B

Derivation of Eqs. (19) and (20) are as follows:

$|h_1|^2, |h_{pu_1}|^2, |h_2|^2$ and $|h_{pu_2}|^2$ respectively subjects to independent and identically exponential distribution with rate parameter $\Omega_1, \Omega_{pu_1}, \Omega_2$ and Ω_{pu_2} respectively. For brevity, we define $g_1 = \frac{\gamma_S |h_1|^2}{\gamma_P |h_{pu_1}|^2}$

and $g_2 = \frac{\gamma_S |h_2|^2}{\gamma_P |h_{pu_2}|^2}$ here, the probability can be expressed as $f(x)$ and $f(y)$. In addition, we have $c = \frac{a_1}{a_2}, \Delta_1 = \frac{\gamma_{th}}{a_2 \gamma_S}, \Delta_2 = \frac{\gamma_{th}}{(a_1 - a_2 \gamma_{th}) \gamma_S}$. Thus, the outage probability under the condition of $g_1 < g_2$ can be expressed as:

$$\begin{aligned}
 P_{g_1 < g_2}^{u_1} &= 1 - \Pr\{\gamma_1 > \gamma_{th}, g_1 < g_2\} \\
 &= 1 - \Pr\left\{\frac{a_1 g_1}{a_2 g_2 + 1} > \gamma_{th}, g_1 < g_2\right\} \\
 &= 1 - \Pr\left\{g_1 > \frac{\gamma_{th}}{a_1 - a_1 \gamma_{th}}, g_1 < g_2\right\} \\
 &= 1 - \int_{\Delta_2}^{+\infty} f_{g_1}(x) dx \int_0^y f_{g_2}(y) dy, c > \gamma_{th}
 \end{aligned} \tag{30}$$

$$\begin{aligned}
 P_{g_1 < g_2}^{u_2} &= 1 - \Pr\{\gamma_2 > \gamma_{th}, \gamma_{2 \rightarrow 1} > \gamma_{th}, g_1 < g_2\} \\
 &= 1 - \Pr\{a_2 g_2 > \gamma_{th}, \frac{a_1 g_1}{a_2 g_2 + 1} > \gamma_{th}, g_1 < g_2\} \\
 &= 1 - \Pr\{g_2 > \frac{\gamma_{th}}{a_2 \gamma_s}, g_2 > \frac{\gamma_{th}}{(a_1 - a_2 \gamma_{th}) \gamma_s}, x < y\} \\
 &= \begin{cases} 1 - \int_{\Delta_1}^{+\infty} f_{g_2}(x) dx \int_0^x f_{g_1}(y) dy, c > \gamma_{th} + 1 \\ 1 - \int_{\Delta_2}^{+\infty} f_{g_2}(x) dx \int_0^x f_{g_1}(y) dy, \gamma_{th} < c < \gamma_{th} + 1 \end{cases} \tag{31}
 \end{aligned}$$

where $f_{g_1}(x) = \frac{\gamma_S \gamma_P \Omega_1 \Omega_{pu_1}}{(\gamma_S \Omega_1 + x \gamma_P \Omega_{pu_1})^2}$, $f_{g_2}(y) = \frac{\gamma_S \gamma_P \Omega_2 \Omega_{pu_2}}{(\gamma_S \Omega_2 + y \gamma_P \Omega_{pu_2})^2}$.

If $c > \gamma_{th} + 1$, $P_{g_1 < g_2}^{u_2}$ is given as:

$$\begin{aligned}
 P_{g_1 < g_2}^{u_2} &= 1 - \int_{\Delta_1}^{+\infty} f_{g_2}(y) dy \int_0^y f_{g_1}(x) dx \\
 &= 1 - \int_{\frac{\gamma_{th}}{a_2 \gamma_s}}^{+\infty} \frac{\gamma_S \gamma_P \Omega_2 \Omega_{pu_2}}{(\gamma_S \Omega_2 + y \gamma_P \Omega_{pu_2})^2} dy \int_0^{\frac{a_2 \gamma_S y - \gamma_{th}}{\gamma_{th} \gamma_P}} \frac{\gamma_S \gamma_P \Omega_1 \Omega_{pu_1}}{(\gamma_S \Omega_1 + x \gamma_P \Omega_{pu_1})^2} dx \\
 &= 1 - (b_1 b_2 \ln(1 - \frac{z_2}{b_1}) + z_2 b_1). \tag{32}
 \end{aligned}$$

Else, $\gamma_{th} < c < \gamma_{th} + 1$, $P_{g_1 < g_2}^{u_2}$ can be calculated as

$$\begin{aligned}
 P_{g_1 < g_2}^{u_2} &= 1 - \int_{\Delta_1}^{+\infty} f_{g_2}(y) dy \int_0^y f_{g_1}(x) dx \\
 &= 1 - \int_{\frac{\gamma_{th}}{(a_1 - a_2 \gamma_{th}) \gamma_s}}^{+\infty} \frac{\gamma_S \gamma_P \Omega_2 \Omega_{pu_2}}{(\gamma_S \Omega_2 + y \gamma_P \Omega_{pu_2})^2} dy \int_0^{\frac{(a_1 - a_2 \gamma_{th}) \gamma_S y - \gamma_{th}}{\gamma_{th} \gamma_P}} \frac{\gamma_S \gamma_P \Omega_1 \Omega_{pu_1}}{(\gamma_S \Omega_1 + x \gamma_P \Omega_{pu_1})^2} dx \\
 &= 1 - (b_1 b_2 \ln(1 - \frac{z_3}{b_1}) + z_3 b_1). \tag{33}
 \end{aligned}$$

Similarly,

$$\begin{aligned}
 P_{g_1 > g_2}^{u_1} &= 1 - \int_{\Delta_1}^{+\infty} f_{g_2}(y) dy \int_0^y f_{g_2}(y) dy \\
 &= 1 - \int_{\frac{\gamma_{th}}{(a_1 - a_2 \gamma_{th}) \gamma_S}}^{+\infty} \frac{\gamma_S \gamma_P \Omega_1 \Omega_{pu_1}}{(\gamma_S \Omega_1 + x \gamma_P \Omega_{pu_1})^2} dx \int_0^{\frac{(a_1 - a_2 \gamma_{th}) \gamma_S x - \gamma_{th}}{\gamma_{th} \gamma_P}} \frac{\gamma_S \gamma_P \Omega_2 \Omega_{pu_2}}{(\gamma_S \Omega_2 + y \gamma_P \Omega_{pu_2})^2} dy \\
 &= 1 - (z_1 b_1 - b_1 b_2 \ln(1 + \frac{z_1}{b_2}))
 \end{aligned} \tag{34}$$

For simplicity, we have

$$\begin{aligned}
 b_1 &= \frac{\Omega_2 \Omega_{pu_1}}{\Omega_2 \Omega_{pu_1} - \Omega_1 \Omega_{pu_2}} \\
 b_2 &= \frac{\Omega_1 \Omega_{pu_2}}{\Omega_2 \Omega_{pu_1} - \Omega_1 \Omega_{pu_2}} \\
 z_1 &= \frac{(a_1 - \gamma_{th} a_2) \gamma_S \Omega_1}{(a_1 - \gamma_{th} a_2) \gamma_S \Omega_1 + \gamma_{th} \gamma_P \Omega_{pu_1}} \\
 z_2 &= \frac{a_2 \gamma_S \Omega_2}{a_2 \gamma_S \Omega_2 + \gamma_{th} \gamma_P \Omega_{pu_2}} \\
 z_3 &= \frac{(a_1 - \gamma_{th} a_2) \gamma_S \Omega_2}{(a_1 - \gamma_{th} a_2) \gamma_S \Omega_2 + \gamma_{th} \gamma_P \Omega_{pu_2}}
 \end{aligned}$$

In summary, the outage probability of secondary users can be written as:

$$P_{g_1 < g_2}^{u_1} = 1 - (b_1 b_2 \ln(1 + \frac{z_1}{b_2}) - z_1 b_1), c > \gamma_{th} \tag{35}$$

$$P_{g_1 < g_2}^{u_2} = \begin{cases} 1 - (b_1 b_2 \ln(1 - \frac{z_2}{b_1}) + z_2 b_1), c > \gamma_{th} + 1 \\ 1 - (b_1 b_2 \ln(1 - \frac{z_3}{b_1}) + z_3 b_1), \gamma_{th} < c \gamma_{th} + 1 \end{cases} \tag{36}$$